The atmospheric carbon capture performance of legacy iron and steel waste

SUPPORTING INFORMATION

Huw Pullin,[*,†] *Andrew W. Bray*[‡], *Ian T. Burke,*[‡] *Duncan D. Muir,*[†] *Devin J. Sapsford,*[§] *William M. Mayes*[‖] *and Phil Renforth*[∇]

†School of Earth and Ocean Sciences, Cardiff University, Cardiff, CF10 3AT, UK

‡School of Earth and Environment, University of Leeds, Leeds, LS2 9JT, UK

§School of Engineering, Cardiff University, Cardiff, CF24 78 3AA, UK

‖Department of Geography, Geology and Environment, University of Hull, Hull, HU6 7RX, UK

∇School of Engineering and Physical Sciences, Heriot-Watt University, Edinburgh, EH14 4AS, UK

***Corresponding author:** PullinH2@cardiff.ac.uk

Pages: 21

Figures: 8

Tables: 6

Table S1. Common minerals in iron and steel slag samples as identified in academic literature

Mineral Name	Formula	Mineral Group	CN*	Notes
Silicates				
Dicalcium silicate[1-44]	Ca_2SiO_4	Olivine	C_2S	Includes β- (larnite) and γ- (belite) phases
Tricalcium silicate[2, 8, 12, 16, 19-25, 27, 30, 33-35, 37-40, 42, 45]	Ca_3SiO_5		C_3S	Includes alite and haturite
Akermanite[2, 13, 18, 21, 36, 43, 46, 47]	$Ca_2MgSi_2O_7$	Melilite	C_2MS_2	
Merwinite[1, 14, 17, 18, 21, 32, 33, 35, 37, 40, 42, 43, 47, 48]	$Ca_3Mg(SiO_4)_2$		C_3MS_2	
Gehlenite[2, 11, 13, 14, 18, 21, 26, 28, 31, 33-35, 37, 39, 40, 43, 44, 46-50]	$Ca_2Al_2SiO_7$	Melilite		
Quartz[1, 13, 15, 21, 34, 39, 48, 50-52]	SiO_2	Quartz		
Christobalite[51, 52]	SiO_2	Quartz		
Fayalite[3, 9, 31, 38, 52]	Fe_2SiO_4	Olivine		Includes divalent substitution
Kushiroite[49]	$CaAl_2SiO_6$	Pyroxene	MS	
Enstatite[2, 3, 12, 21, 38, 42, 48, 53]	$MgSiO_3$	Pyroxene		
Wollastonite[3, 9, 17, 25, 42, 54]	$CaSiO_3$	Pyroxenoid	CS	
Ferrosilicate[3]	$FeSiO_3$			
Ferrosilite[9, 52]	$Fe_2Si_2O_6$	Pyroxene		Includes divalent cation substitution
Calcium magnesium aluminium iron silicate[14]	$Ca_2MgOAlFeSiO_5$			
Clinoenstatite[9]	$Mg_2Si_2O_6$			
Diopside[21, 30, 42, 49, 50]	$MgCaSi_2O_6$	Pyroxene	CMS_2	
Forsterite[38]	Mg_2SiO_4	Olivine		
Monticellite[17, 21, 40, 42, 43]	$CaMgSiO_4$		CMS	
Cuspidine[14]	$Ca_4Si_2O_7F_2$	Sorosilicate		
Mullite[52]	$Al_6Si_2O_{13}$			
Plagioclase[52]	$CaAl_2Si_2O_8$–$NaAlSi_3O_8$			
Bredigite[20, 21, 28-30]	$Ca_{12}Al_{14}O_{33}$ $Ca_{14}Mg_2(SiO_4)_8$			
Alkali feldspar[52]	$KAlSi_3O_8$	Feldspar		
Anorthite[31, 37, 43]	$CaAl_2Si_2O_8$	Plagioclase		
Iscorite[31]	Fe_7SiO_{10}			
Dicalcium iron magnesium silicate[33]	$Ca_2Fe_{1.2}Mg_{0.4}Si_{0.4}O_5$			
Zircon[52]	$ZrSiO_4$	Zircon		
Andradite[52]	$Ca_3(FeTi)_2Si_3O_{12}$	Garnet		
Rankinite[42]	$Ca_3Si_2O_7$		C_3S_2	
Oxides				
Periclase[2, 3, 8, 13-15, 17, 19, 21, 27, 30, 32, 34-39, 42]	MgO			
Lime[1, 3, 5, 8, 9, 15-17, 19-21, 24, 27, 31, 32, 38, 42, 55, 56]	CaO			
Wüstite[2, 3, 5, 6, 8-10, 12, 14, 15, 19-21, 24-26, 29, 31, 34, 36, 38, 39, 42, 44, 45, 53, 55]	FeO			
Corundum[2, 4, 9, 12, 18, 29, 31, 36]	α-Al_2O_3			
Hematite[1, 3, 8, 17, 23, 24, 31, 33, 52, 56]	Fe_2O_3	Iron oxides		
Magnetite[1-4, 12-15, 18, 20, 21, 26, 28, 29, 34, 35, 38-40, 42, 44, 53]	Fe_3O_4	Iron oxides		Includes maghemite
Spinel[27, 30, 35, 48, 50, 52]	$MgAl_2O_4$			Includes multivalent substitution
Magnesioferrite[20, 28, 37]	$MgFe_2O_4$		MF	

Calcium ferrite[1, 3, 5, 7-9, 14-20, 23, 24, 27, 32-38, 41, 42, 45, 55]	$Ca_2Fe_2O_5$ (srebrodolskite) or $CaFe_2O_4$		CF	Includes multivalent cation substitution
Hercynite[14]	$FeAl_2O_4$			
Brownmillerite[6, 12, 21, 39, 40, 56]	Ca_2FeAlO_5		C_4AF	
Manganese oxides[14, 28, 31]	MnO_2 or Mn_3O_4			
RO phases (mixed oxides)[4, 7, 10, 12-14, 19, 21, 24, 27, 32, 35-38, 42, 52, 53, 55]	Various solid solutions			
Calcium aluminium oxides[2, 13, 14, 20-22, 34, 35, 38, 39, 42, 44]	$CaAl_2O_3$ or $Ca_3Al_2O_6$ or $Ca_{12}Al_{14}O_{33}$ (mayenite)			
Hydroxides				
Portlandite[1, 2, 4, 5, 7, 9, 10, 12, 14, 15, 17, 21-24, 27, 30, 37, 53, 55, 57]	$Ca(OH)_2$		CH	
Brucite[2, 4, 9]	$Mg(OH)_2$		MH	
Goethite[52]	FeOOH			
Carbonates				
Calcite[1, 2, 4, 5, 7, 11, 12, 15, 17, 20, 23-25, 27, 37, 38, 51-53, 58]	$CaCO_3$			Includes Mn cation substitution
Aragonite[5, 53]	$CaCO_3$			
Dolomite[17, 49, 51]	$CaMg(CO_3)_2$			
Magnesite[17]	$MgCO_3$			
Ankerite[53]	$Ca(FeMgMn)(CO_3)_2$			
Kutnohorite[53]	$Ca(MnMgFe)(CO_3)_2$			
Tilleyite[40]	$Ca_2Si_2O_7(CO_3)_2$			
Sulphides and sulphates				
Oldhamite[31, 47, 49, 52]	(CaMg)S			Includes divalent cation substitution
Gypsum/Anhydrite[11, 30]	$CaSO_4$			
Iron sulphide[42, 52]	FeS			
Magnesium sulphate[17]	$MgSO_4 \cdot 5H_2O$			
Ettringite[11]	$Ca_6Al_2OH_{12}(SO_4)_3 \cdot 26H_2O$			
Others				
Metallic iron[3, 5, 21, 38, 47, 49, 52, 55]	Fe	Metals		
Fluorite[13, 21]	CaF_2	Halite		
Graphite[52]	C			
Whitlockite[33]	$Ca_3(PO_4)_2$	Phosphates		
Calcium dihydrogen phosphate[33]	$Ca(H_2PO_4)_2 \cdot H_2O$	Phosphates		

* - Cement Notation

Figure S1. Photographs of the drilling works on site at Consett

Figure S2. Photographs of the material recovered from Consett

S1. Details of sample analysis

S1.1 Preparation

All slag samples were oven dried at 105 °C. Particle size distribution (PSD) analysis on bulk samples was performed using sieves in accordance with BS ISO 11277:2009. [51] To prepare for X-ray diffraction (XRD), X-ray fluorescence (XRF), acid digestion elemental inductively coupled plasma-optical emission spectroscopy (ICP-OES), total carbon (TC) and total organic carbon (TOC) analysis, samples were pulverised using a Siebtechnik vibrating-puck mill with a tungsten carbide grinding bowl. until a homogenous powder was obtained. Equipment was washed using distilled water and acetone between samples. All powdered samples were stored in plastic, sealable bags until analysed. To prepare for microscopy, selected samples were mounted in resin blocks, before being ground and polished with a sol-gel alumina (Al_2O_3) suspension to a 0.25 μm finish. Before scanning electron microscopy analysis, the samples were coated with 15 – 20 nm carbon (C) by thermal evaporation.

S1.2 Sample analysis

X-ray diffraction was performed by placing powders into aluminium (Al) holders, then analysing with a copper (Cu) *Kα* radiation source operating at 35 kV and 40 mA. Samples were scanned from 5 to 55 °2θ, at a step size of 0.02 °2θ, with a counting time of 1 s per step. At Cardiff University, a Philips PW1710 Automate Powder Diffractomer was used, and diffraction patterns were analysed using PW1876 PC-Identify software, version 1.0b, and also compared with JCPDS cards of standard materials. At the University of Leeds, a Bruker D8 diffractometer was used, and diffraction patterns were analysed using the EVA® software using the ICDD PDF2 database. Semi-quantitative elemental analysis by XRF was carried out on an Olympus X-5000 instrument on pressed, powdered samples in the laboratory at Cardiff University. Accuracy of the XRF data was determined to be on average ±6.7% by the analysis

of silicate rich reference materials (Certified Reference Material: Stream Sediment STSD-1 and STSD-4 from Canmet Mining and Mineral Sciences, Ottawa, Canada) (Table S2). Total carbon (TC) and sulphur measurements were performed on a Leco SC-144DR S/C (sulphur/carbon) analyser at 1350 °C in a pure (>99.9 %) oxygen (O_2) atmosphere. Total organic carbon (TOC) measurements were performed using a Shimadzu TOC-L total organic carbon analyser using phosphoric acid digestion. For both TC and TOC analysis, Leco calibration samples were run prior to analysis to assess instrument accuracy. Twelve samples were digested and analysed by ICP-OES via a 4 acid digest method (EPA, 1996), [52] (for sample details, see Table S3). Briefly, 0.1 g of sample was placed in a PTFE lined microwave digest cell and 2 mL of analytical grade 45.71 % hydrofluoric acid (HF) was added. This was allowed to stand for 12 hrs, then 6 mL of aqua regia solution (1:1 ratio of analytical grade 32 % hydrochloric acid (HCl) and 70 % nitric acid (HNO_3)) was added, and then microwave digested using an Anton Paar Multiwave 3000, at 200 °C (1400 W) for 30 minutes (after a 10 minute up ramp time period). After a 15 minute cooling period, the resultant solution was neutralised by adding 12 mL of analytical grade 4 % boric acid (H_3BO_3), and then microwave digested at 150 °C (900 W) for 20 minutes (after a 5 minute ramp-up time period). After a further 15 minute cooling period, the sample was analysed by inductively coupled plasma-optical emission spectroscopy (ICP-OES) using a Perkin Elmer Optima 2100 DV instrument. Calibration standards (20, 40, 60, 80 and 100 mg/L) were prepared in 1% nitric acid from 1000 mg/L ICP standards. Experimental blanks and elemental standards at 50 mg/L were analysed to check for accuracy and instrumental drift. Accuracy of the ICP data was determined to be on average ±3.6 % by the analysis of silicate rich reference materials (Certified Reference Material: Stream Sediment STSD-1 from Canmet Mining and Mineral Sciences, Ottawa, Canada) (Table S2). Selected samples from each borehole were chosen for scanning electron microscopy-energy dispersive X-ray spectroscopy (SEM-EDS) analysis (for sample details,

see Table S3). At Cardiff University, SEM analyses were performed using a FEI-XL30 FEG-ESEM under high vacuum conditions. A beam energy of 15 keV was used with a 50 μm diameter final aperture with a nominal beam current of ~1 nA and a 10 mm working distance. EDS spectra were acquired using a 10 mm^2 Oxford Instruments X-Act silicon (Si) drift detector with Inca software with a 20 s livetime and a deadtime of less than 10 %. All totals were normalised to 100 %. At the University of Leeds, SEM analyses were performed using a Tescan VEGA3 XM equipped with an X-max 150 SDD EDS and Aztec 3.3 software. A beam energy of 15 keV was used, with a 15 mm working distance, mapping at a resolution of 2 μm. All totals were normalised to 100 %.

Table S2. Comparison of recorded XRF elemental wt% concentrations (mg/kg) against known standards (Certified Reference Material: Stream Sediment STSD-1 and STSD-4 from Canmet Mining and Mineral Sciences, Ottawa, Canada)

			STSD-1 (mg/kg)		
Element	**Si**	**K**	**Ca**	**Mn**	**Fe**
Standard	22.493	0.996	1.905	0.387	4.456
1.	21.140	1.101	2.125	0.419	4.701
2.	20.240	1.077	2.082	0.409	4.715
3.	20.870	1.097	2.039	0.411	4.775
Mean	20.750±0.462	1.092±0.013	2.082±0.043	0.413±0.01	4.730±0.039
% Difference	-7.7	9.6	9.2	6.8	4.1
			STSD-4 (mg/kg)		
Element	**Si**	**K**	**Ca**	**Mn**	**Fe**
Standard	27.532	1.328	2.859	0.155	3.987
1.	25.67	1.392	3.078	0.166	4.312
2.	25.60	1.397	3.061	0.168	4.361
3.	25.67	1.385	3.064	0.168	4.382
Mean	25.648±0.0038	1.391±0.006	3.068±0.0094	0.167±0.001	4.352±0.036
% Difference	-3.8	4.8	7.3	8.0	9.1

Table S3. Details of samples depths analysed by ICP-OES and SEM

Borehole	ICP-OES	SEM-EDX
BH 1	8.25	2.25
	20.25	10.25
	22.25	16.0
	23.75	
BH 2	4.25	12.5
	10.25	18.5
	14.25	
	16.25	
BH 3	2.25	4.25
	6.25	16.25
	12.25	
	18.25	

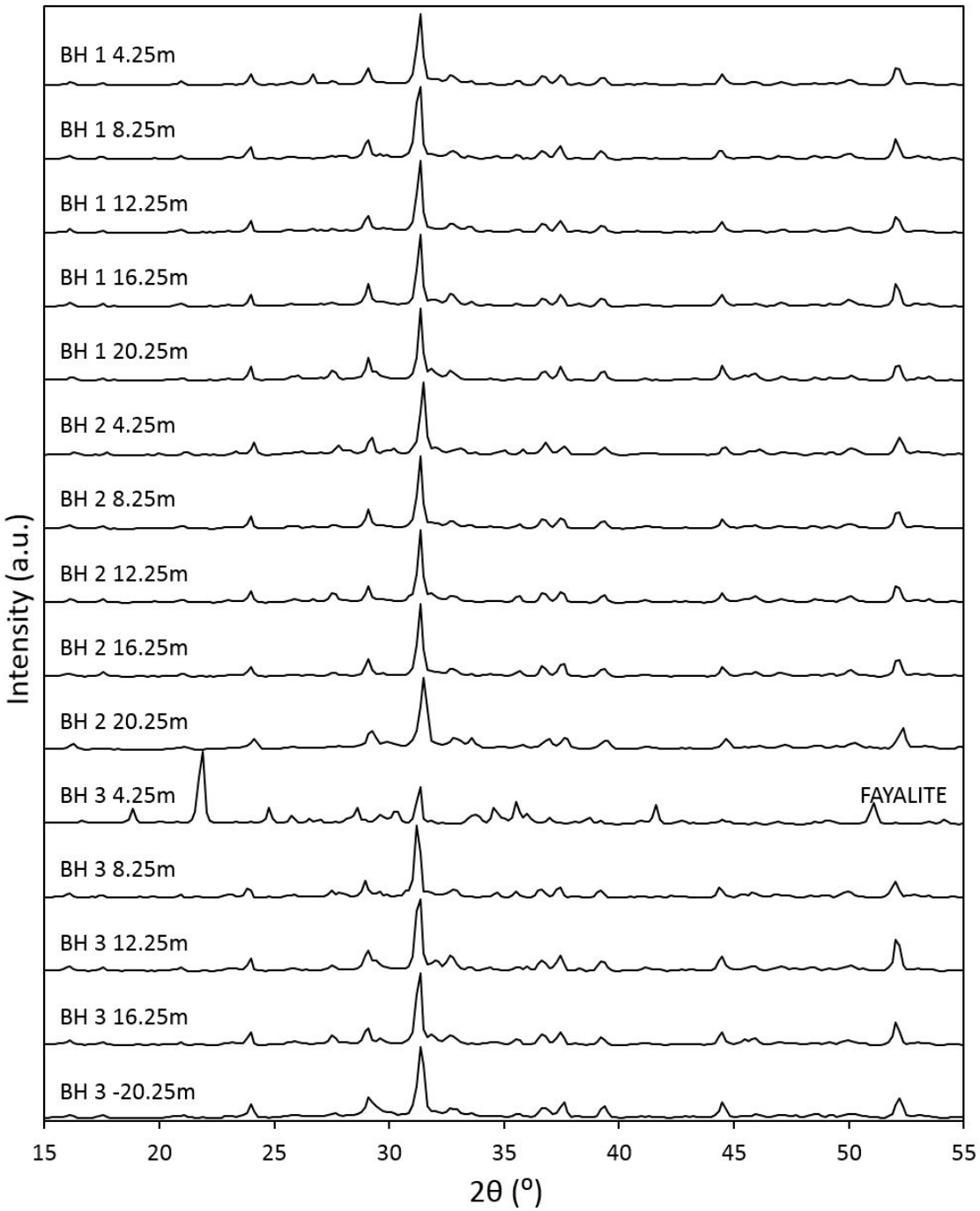

Figure S3. Slag diffractogram plots from BH 1, BH 2 and BH 3 at various depths

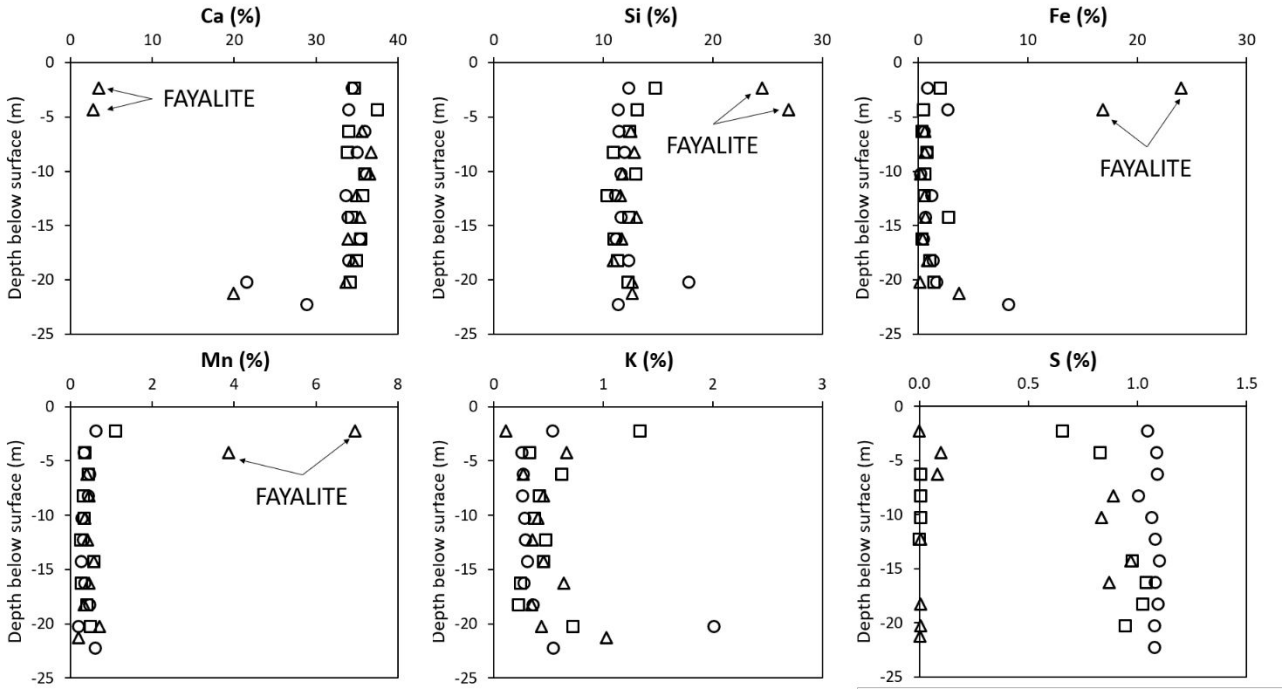

Figure S4. Semi-quantitative elemental analysis of slag material by XRF, except S (using furnace analysis)

Key: **Circle** – BH 1, **Square** – BH 2, **Triangle** – BH 3

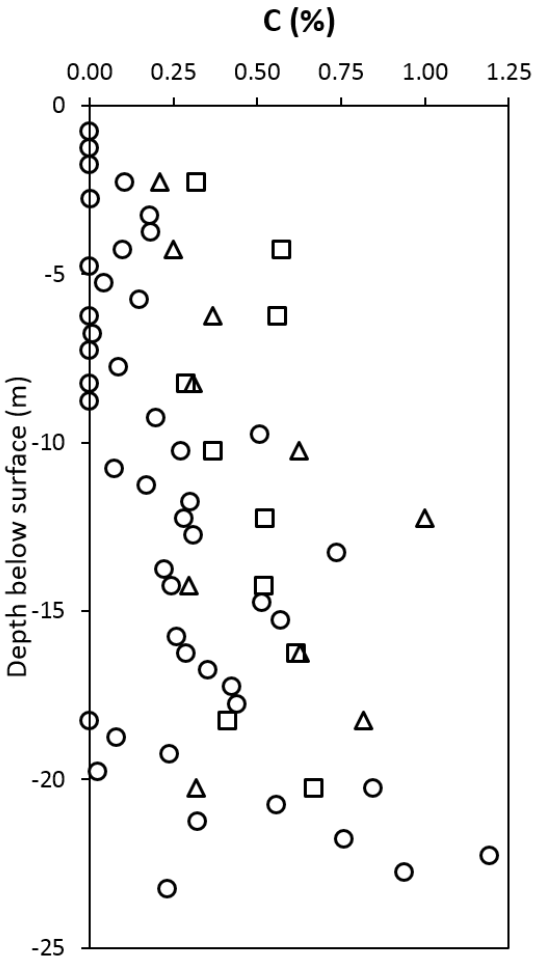

Figure S5. Total carbon concentrations of slag material (via furnace analysis) plotted against depth

Key: **Circle** – BH 1, **Square** – BH 2, **Triangle** – BH

Table S4: Analysis of borehole samples by HF digestion ICP-OES with known standard material (Certified Reference Material: Stream Sediment STSD-1 from Canmet Mining and Mineral Sciences, Ottawa, Canada)

			Concentration (mg/kg)													
			Na	**Ca**	**Mg**	**Si**	**K**	**Fe**	**Al**	**Mn**	**S**	**Ba**	**Sr**	**Ti**	**Zn**	**P**
BH 1	**8.25**	**Slag**	2659	283517	18799	213704	1887	5626	57750	4894	8276	974	1142	1486	65	104
	20.25	**Slag**	4513	287328	7095	176875	3416	9138	45388	3241	13138	5251	1170	1404	88	35
	22.25	**Slag**	5692	327550	13177	143574	3565	103980	56112	8990	11641	1646	1568	1670	93	32
	23.75	**Clay**	11724	18351	1850	339033	9218	25350	45003	501	4461	372	184	3562	170	347
BH 2	**4.25**	**Slag**	5652	373198	13952	174423	2792	4801	64068	6122	6598	1537	1489	1797	52	11
	10.25	**Slag**	3347	283069	14959	168147	2393	5179	48282	4063	9679	1111	1605	1656	43	17
	14.25	**Slag**	3713	332455	22902	141481	3285	44822	66405	9087	11065	1962	1790	1571	43	45
	16.25	**Slag**	3255	326317	25890	138728	1799	2667	52216	3890	17548	976	1409	1286	27	43
BH 3	**2.25**	**Fayalite**	14115	25997	1797	219154	1755	254148	11061	104433	906	4113	145	5285	51	0
	6.25	**Slag**	2625	291799	20001	179643	1992	5888	61990	6419	11579	2953	1708	1822	26	53
	12.25	**Slag**	5394	386777	19170	201957	2978	5890	59392	6727	13756	3230	1808	1808	31	39
	18.25	**Slag**	3459	350583	18939	159025	2718	14145	67563	5141	18652	942	1344	1542	21	46
	STSD-1	**Standard**	13353	25729	13267	198672	9962	45464	47632	3872	721	630	170	4600	178	1746
		Measured	13684	25030	13939	208823	9932	44534	46145	3759	691	659	161	4567	188	1758
		Accuracy	2.5	-2.7	5.1	-5.0	-6.4	-2.0	-3.1	-2.9	-4.1	4.6	-5.3	-0.7	5.6	0.7

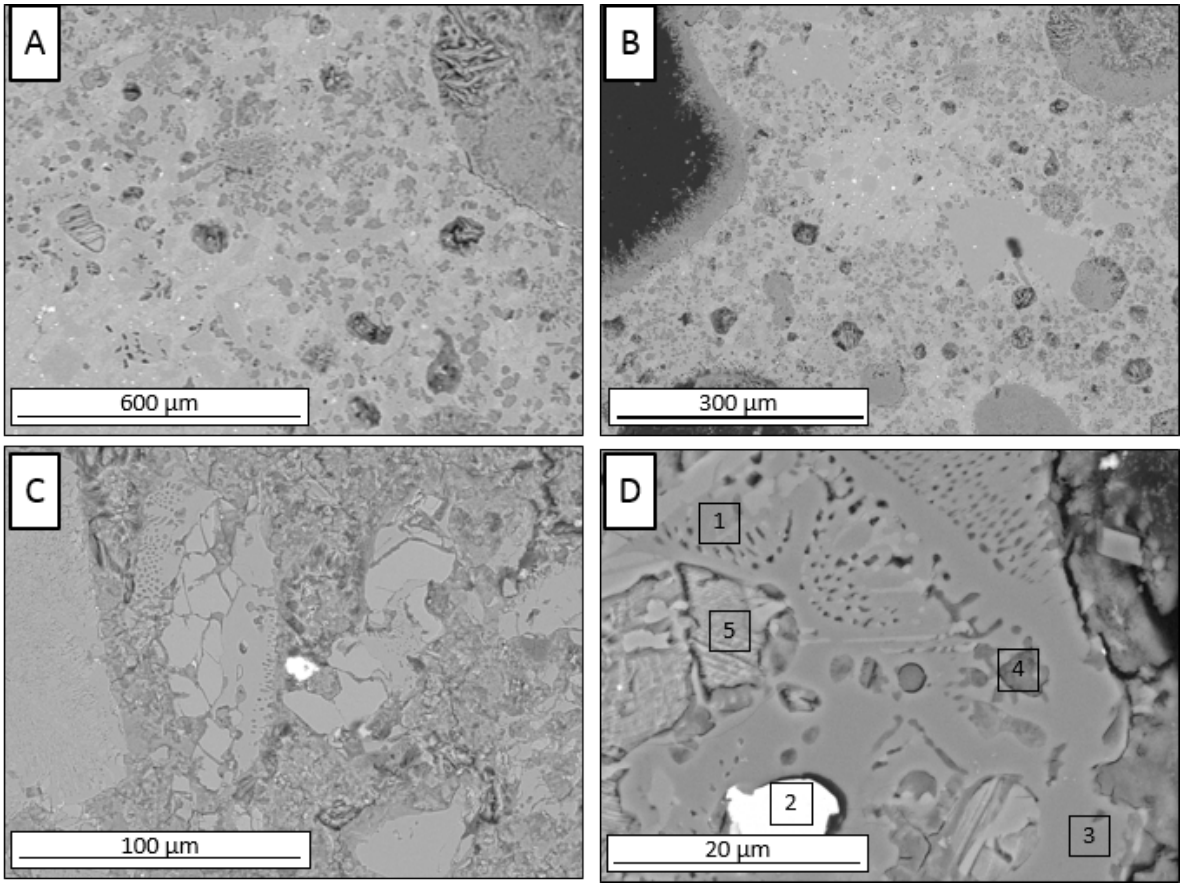

Figure S6: BSE images of typical slag material, from BH 1 at 4.5 m

Table S5: Semi-quantitative phase composition in slag sample from BH 1 (4.5 m depth) by SEM-EDS spot analysis. Numbers refer to areas mapped in Figure S5 D

Element	1. 'Melilite' Atom %±1σ	2. 'Fe- metal (oxidised)' Atom %±1σ	3. 'Melilite' Atom %±1σ	4. 'Melilite' Atom %±1σ	5. 'Larnite' Atom %±1σ
Mg	2.8	n.d.*	2.6	2.6	0.4
Al	5.3	n.d.*	7.7	7.7	n.d.*
Si	8.8	n.d.*	9.3	9.0	9.7
S	0.7	n.d.*	n.d.*	n.d.*	n.d.*
Ca	25.9	1.6	23.9	27.2	35.1
Fe	n.d.*	48.4	n.d.*	n.d.*	n.d.*
O	56.5	50.0	56.6	56.4	54.8

*not detected n, number of EDS spectra

Note: mineral names are inferred and are not definitive.

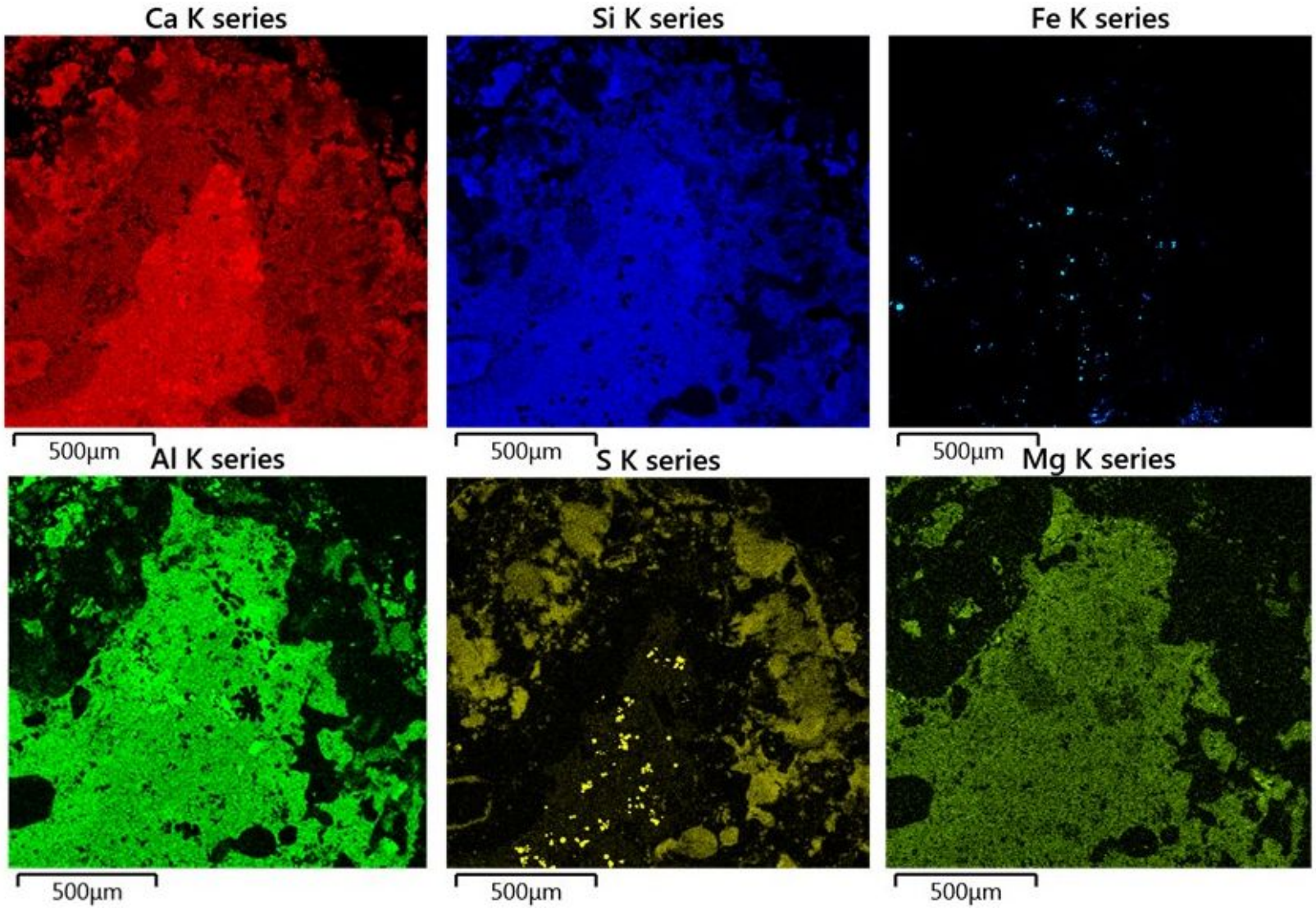

Figure S7. SEM-EDS elemental maps for major elements present in the slag sample shown in Figure 3

Table S6. Semi-quantitative phase composition in slag sample from BH 1 (16m depth) by SEM-EDS spot analysis. Number refer to spots in Figure 3C) (1 - 5) and Figure 3D) (6 - 8)

Element	1. 'Fe-metal' n = 1 Atom %±1σ	2. 'CaS' n = 5 Atom % ±1σ	3. 'Larnite' n = 6 Atom % ±1σ	4. 'Melilite' n = 6 Atom % ±1σ	5. 'Melilite' n = 5 Atom % ±1σ	6. 'Amphorous' Ca-Si-H' n = 5 Atom % ±1σ	7. 'Blocky Ettringite' n = 4 Atom % ±1σ	8. 'Needle Thaumasite' n = 5 Atom % ±1σ
O	n.d.*	17 ±3	58 ±0.3	59 ±0.2	60 ±0.4	70 ±2	74 ±1	72 ±2
Na	n.d.*	0.7 ±0.70	n.d.*	n.d.*	n.d.*	n.d.*	n.d.*	n.d.*
Mg	n.d.*	n.d.*	1.0 ±0.02	1.4 ±0.05	3.4 ±0.5	0.6 ±0.8	n.d.*	n.d.*
Al	n.d.*	n.d.*	0.2 ±0.4	14 ±0.4	8.4 ±0.5	n.d.*	4.5 ±0.5	0.6 ±0.1
Si	n.d.*	n.d.*	14 ±0.1	9.7 ±0.1	9.7 ±0.1	7.5 ±1.8	0.3 ±0.2	4.7 ±1.2
S	n.d.*	42 ±1	n.d.*	n.d.*	n.d.*	0.2 ±0.1	7.4 ±0.4	8.0 ±1.7
Ca	1.3	41 ±2	27 ±0.5	17±0.3	16 ±0.1	20 ±1.4	14 ±1	14 ±1
Mn	n.d.*	0.4 ±0.03	n.d.*	n.d.*	0.1 ±0.1	n.d.*	n.d.*	n.d.*
Fe	98.7	n.d.*	n.d.*	n.d.*	n.d.*	n.d.*	n.d.*	n.d.*
Ca/Si	n.a.	n.a.	1.91 ±0.02	1.73 ±0.02	1.29 ±0.02	2.8 ±0.8		3.2 ±0.6
Ca/Al	n.a.						3.0 ±0.2	-
Ca/S	n.a.						1.9 ±0.1	1.9 ±0.5

*not detected n, number of EDS spectra

Note: mineral names are inferred and are not definitive.

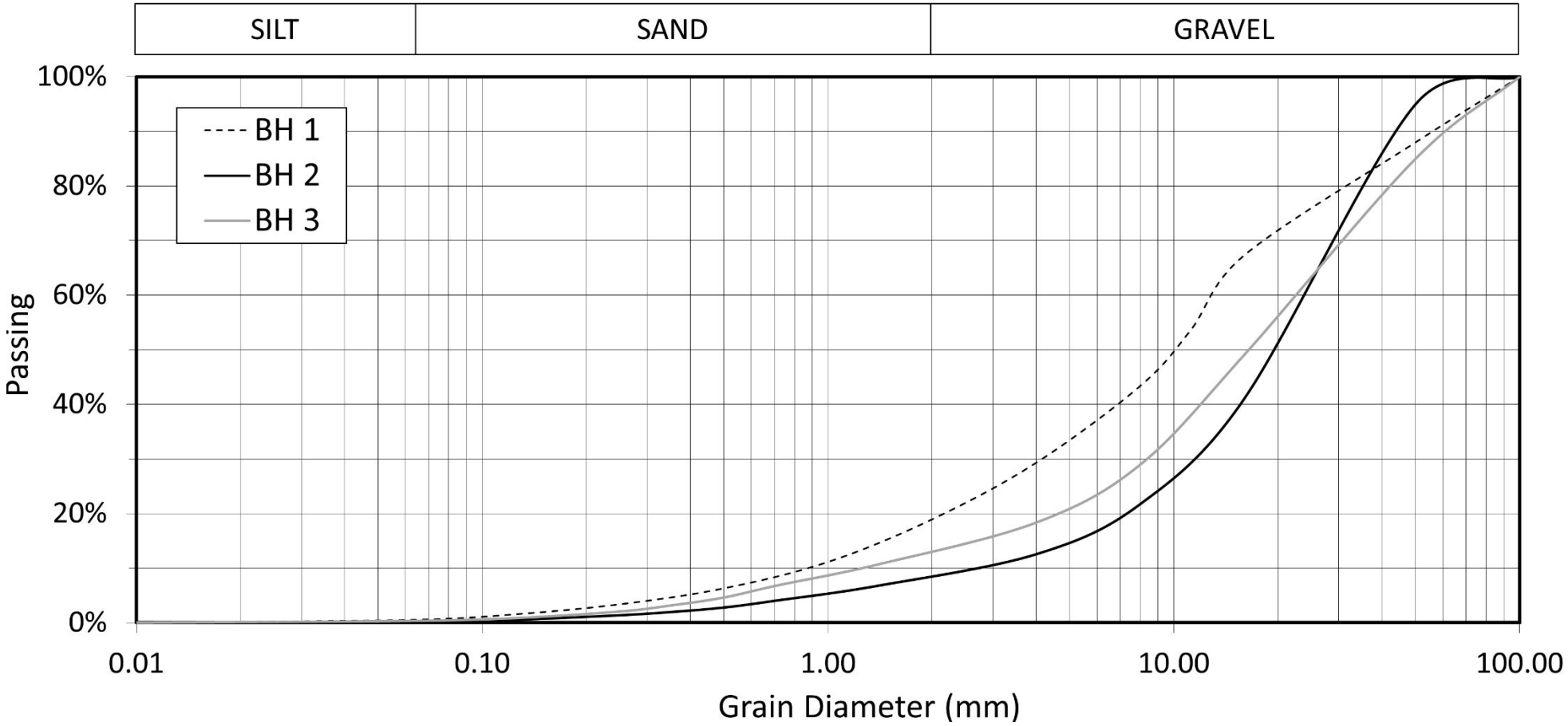

Figure S8: Averaged particle size distribution curves for Consett slag material

References

1. Navarro, C.; Díaz, M.; Villa-García, M. A., Physico-Chemical Characterization of Steel Slag. Study of its Behavior Under Simulated Environmental Conditions. *Environmental Science & Technology* **2010,** *44*, (14), 5383-5388.
2. Baciocchi, R.; Costa, G.; Di Gianfilippo, M.; Polettini, A.; Pomi, R.; Stramazzo, A., Thin-film versus slurry-phase carbonation of steel slag: CO2 uptake and effects on mineralogy. *Journal of Hazardous Materials* **2015,** *283*, 302-313.
3. Santos, R. M.; Ling, D.; Sarvaramini, A.; Guo, M.; Elsen, J.; Larachi, F.; Beaudoin, G.; Blanpain, B.; Van Gerven, T., Stabilization of basic oxygen furnace slag by hot-stage carbonation treatment. *Chemical Engineering Journal* **2012,** *203*, 239-250.
4. Morone, M.; Costa, G.; Polettini, A.; Pomi, R.; Baciocchi, R., Valorization of steel slag by a combined carbonation and granulation treatment. *Minerals Engineering* **2014,** *59*, 82-90.
5. Su, T.-H.; Yang, H.-J.; Shau, Y.-H.; Takazawa, E.; Lee, Y.-C., CO2 sequestration utilizing basic-oxygen furnace slag: Controlling factors, reaction mechanisms and V–Cr concerns. *Journal of Environmental Sciences* **2016,** *41*, 99-111.
6. Polettini, A.; Pomi, R.; Stramazzo, A., CO2 sequestration through aqueous accelerated carbonation of BOF slag: A factorial study of parameters effects. *Journal of Environmental Management* **2016,** *167*, 185-195.
7. Chaurand, P.; Rose, J.; Briois, V.; Olivi, L.; Hazemann, J.-L.; Proux, O.; Domas, J.; Bottero, J.-Y., Environmental impacts of steel slag reused in road construction: A crystallographic and molecular (XANES) approach. *Journal of Hazardous Materials* **2007,** *139*, (3), 537-542.
8. Gautier, M.; Poirier, J.; Bodénan, F.; Franceschini, G.; Véron, E., Basic oxygen furnace (BOF) slag cooling: Laboratory characteristics and prediction calculations. *International Journal of Mineral Processing* **2013,** *123*, 94-101.
9. Bodor, M.; Santos, R. M.; Cristea, G.; Salman, M.; Cizer, Ö.; Iacobescu, R. I.; Chiang, Y. W.; van Balen, K.; Vlad, M.; van Gerven, T., Laboratory investigation of carbonated BOF slag used as partial replacement of natural aggregate in cement mortars. *Cement and Concrete Composites* **2016,** *65*, 55-66.
10. Ding, Y.-C.; Cheng, T.-W.; Liu, P.-C.; Lee, W.-H., Study on the treatment of BOF slag to replace fine aggregate in concrete. *Construction and Building Materials* **2017,** *146*, 644-651.
11. Cravotta III, C. A. *Assessment of characteristics and remedial alternatives for abandoned mine drainage: Case study at Staple Bend Tunnel unit of Allegheny Portage Railroad National Historic Site, Cambria County, Pennsylvania, 2004*; 2005-1283; 2005.
12. Costa, G.; Polettini, A.; Pomi, R.; Stramazzo, A., Leaching modelling of slurry-phase carbonated steel slag. *Journal of Hazardous Materials* **2016,** *302*, 415-425.
13. Baciocchi, R.; Costa, G.; Polettini, A.; Pomi, R., Effects of thin-film accelerated carbonation on steel slag leaching. *Journal of Hazardous Materials* **2015,** *286*, 369-378.
14. Gahan, C. S.; Cunha, M. L.; Sandström, Å., Comparative study on different steel slags as neutralising agent in bioleaching. *Hydrometallurgy* **2009,** *95*, (3), 190-197.
15. Belhadj, E.; Diliberto, C.; Lecomte, A., Characterization and activation of Basic Oxygen Furnace slag. *Cement and Concrete Composites* **2012,** *34*, (1), 34-40.
16. Li, Z.; Zhao, S.; Zhao, X.; He, T., Cementitious property modification of basic oxygen furnace steel slag. *Construction and Building Materials* **2013,** *48*, 575-579.

17. Yildirim, I. Z.; Prezzi, M., Chemical, Mineralogical, and Morphological Properties of Steel Slag. *Advances in Civil Engineering* **2011,** *2011*, 13.
18. Wendling, L. A.; Binet, M. T.; Yuan, Z.; Gissi, F.; Koppel, D. J.; Adams, M. S., Geochemical and ecotoxicological assessment of iron- and steel-making slags for potential use in environmental applications. *Environmental Toxicology and Chemistry* **2013,** *32*, (11), 2602-2610.
19. Geiseler, J., Use of steelworks slag in Europe. *Waste Management* **1996,** *16*, (1), 59-63.
20. Brand, A. S.; Roesler, J. R., Steel furnace slag aggregate expansion and hardened concrete properties. *Cement and Concrete Composites* **2015,** *60*, 1-9.
21. Vlcek, J.; Tomkova, V.; Ovcacikova, H.; Ovcacik, F.; Topinkova, M.; Matejka, V., Slags from steel production: Properties and their utilization. *Metallurgica* **2013,** *52*, (3), 329-333.
22. Pang, B.; Zhou, Z.; Xu, H., Utilization of carbonated and granulated steel slag aggregate in concrete. *Construction and Building Materials* **2015,** *84*, 454-467.
23. Han, F.; Zhang, Z.; Wang, D.; Yan, P., Hydration heat evolution and kinetics of blended cement containing steel slag at different temperatures. *Thermochimica Acta* **2015,** *605*, 43-51.
24. Ko, M.-S.; Chen, Y.-L.; Jiang, J.-H., Accelerated carbonation of basic oxygen furnace slag and the effects on its mechanical properties. *Construction and Building Materials* **2015,** *98*, 286-293.
25. Xi, J.-c.; Xiang, X.-d.; Li, C.-h., Process Improvement on the Gradation Uniformity of Steel Slag Asphalt Concrete Aggregate. *Procedia Environmental Sciences* **2016,** *31*, 627-634.
26. Ter Teo, P.; Seman, A. A.; Basu, P.; Sharif, N. M., Characterization of EAF Steel Slag Waste: The Potential Green Resource for Ceramic Tile Production. *Procedia Chemistry* **2016,** *19*, 842-846.
27. Juckes, L. M., The volume stability of modern steelmaking slags. *Mineral Processing and Extractive Metallurgy* **2003,** *112*, (3), 177-197.
28. Luxán, M. P.; Sotolongo, R.; Dorrego, F.; Herrero, E., Characteristics of the slags produced in the fusion of scrap steel by electric arc furnace. *Cement and Concrete Research* **2000,** *30*, (4), 517-519.
29. Abu-Eishah, S. I.; El-Dieb, A. S.; Bedir, M. S., Performance of concrete mixtures made with electric arc furnace (EAF) steel slag aggregate produced in the Arabian Gulf region. *Construction and Building Materials* **2012,** *34*, 249-256.
30. Manso, J. M.; Losañez, M.; Polanco, J. A.; Gonzalez, J. J., Ladle Furnace Slag in Construction. *Journal of Materials in Civil Engineering* **2005,** *17*, (5), 513-518.
31. Nicolae, M.; Irina, V.; Zăman, F., X-ray diffraction analysis of steel slag and blast furnace slag viewing their use for road construction. *UPB Scientific Bulletin Series B* **2007,** *69*, (2), 99-108.
32. Qian, G. R.; Sun, D. D.; Tay, J. H.; Lai, Z. Y., Hydrothermal reaction and autoclave stability of Mg bearing RO phase in steel slag. *British Ceramic Transactions* **2002,** *101*, (4), 159-164.
33. Reddy, A. S.; Pradhan, R. K.; Chandra, S., Utilization of Basic Oxygen Furnace (BOF) slag in the production of a hydraulic cement binder. *International Journal of Mineral Processing* **2006,** *79*, (2), 98-105.
34. Tsakiridis, P. E.; Papadimitriou, G. D.; Tsivilis, S.; Koroneos, C., Utilization of steel slag for Portland cement clinker production. *Journal of Hazardous Materials* **2008,** *152*, (2), 805-811.
35. Tossavainen, M.; Engstrom, F.; Yang, Q.; Menad, N.; Lidstrom Larsson, M.; Bjorkman, B., Characteristics of steel slag under different cooling conditions. *Waste Management* **2007,** *27*, (10), 1335-1344.

36. Hall, C.; Large, D. J.; Adderley, B.; West, H. M., Calcium leaching from waste steelmaking slag: Significance of leachate chemistry and effects on slag grain mineralogy. *Minerals Engineering* **2014,** *65*, 156-162.
37. Li, J.; Yu, Q.; Wei, J.; Zhang, T., Structural characteristics and hydration kinetics of modified steel slag. *Cement and Concrete Research* **2011,** *41*, (3), 324-329.
38. Zhao, J.; Yan, P.; Wang, D., Research on mineral characteristics of converter steel slag and its comprehensive utilization of internal and external recycle. *Journal of Cleaner Production* **2017,** *156*, 50-61.
39. Kourounis, S.; Tsivilis, S.; Tsakiridis, P. E.; Papadimitriou, G. D.; Tsibouki, Z., Properties and hydration of blended cements with steelmaking slag. *Cement and Concrete Research* **2007,** *37*, (6), 815-822.
40. Muhmood, L.; Vitta, S.; Venkateswaran, D., Cementitious and pozzolanic behavior of electric arc furnace steel slags. *Cement and Concrete Research* **2009,** *39*, (2), 102-109.
41. Shen, W.; Zhou, M.; Ma, W.; Hu, J.; Cai, Z., Investigation on the application of steel slag–fly ash–phosphogypsum solidified material as road base material. *Journal of Hazardous Materials* **2009,** *164*, (1), 99-104.
42. Shi, C., Steel Slag — Its Production, Processing, Characteristics, and Cementitious Properties. *Journal of Materials in Civil Engineering* **2004,** *36*, (3), 230-237.
43. Lewis, D. W., Properties and Uses of Iron and Steel Slags. In *Symposium on Slag, National Institute for Transport and Road Research*, National Slag Association: South Africa, 1982; Vol. MF 182-6, p 11.
44. Gelfi, M.; Cornacchia, G.; Roberti, R. In *Investigations on leaching behavior of EAF steel slags*, 6th European Slag Conference (EUROSLAG 2010), Madrid, Spain, 2010; Madrid, Spain, 2010.
45. Wachsmuth, F.; Geiseler, J.; Fix, W.; Koch, K.; Schwerdtfeger, K., Contribution to the Structure of BOF-Slags and its Influence on Their Volume Stability. *Canadian Metallurgical Quarterly* **1981,** *20*, (3), 279-284.
46. Lee, A. R., *Blastfurnace and steel slag: production, properties, and uses*. Wiley: 1974.
47. Scott, P. W.; Critchley, S. R.; Wilkinson, F. C. F., The chemistry and mineralogy of some granulated and pelletized blastfurnace slags. *Mineralogical Magazine* **1986,** *50*, 141-147.
48. Douglas, G. B.; Wendling, L. A.; Coleman, S., Productive use of steelmaking by-product in environmental applications (I): Mineralogy and major and trace element geochemistry. *Minerals Engineering* **2012,** *35*, 49-56.
49. Butler, B. C. M., Al-rich pyroxene and melilite in a blast-furnace slag and a comparison with the Allendre Meteorite. *Mineralogical Magazine* **1977,** *41*, (320), 6.
50. Wendling, L.; Douglas, G.; Coleman, S.; Yuan, Z. *Assessment of the ability of low-cost materials to remove metals and attenuate acidity in contaminated waters*; CSIRO: 2010; p 138.
51. Bayless, E. R.; Greenman, T. K.; Harvey, C. C. *Hydrology and Geochemistry of a Slag-affected Aquifer and Chemical Characteristics of Slag-Affected Ground Water, Northwestern Indiana and Northeastern Illinois*; U.S. Geological Survey: 1998; p 67.
52. Piatak, N. M.; Seal, R. R., Mineralogy and Environmental Geochemistry of Historical Iron Slag, Hopewell Furnace National Historic Site, Pennsylvania, USA. *Applied Geochemistry* **2012,** *27*, (3), 623-643.
53. Polettini, A.; Pomi, R.; Stramazzo, A., Carbon sequestration through accelerated carbonation of BOF slag: Influence of particle size characteristics. *Chemical Engineering Journal* **2016,** *298*, 26-35.

54. Lee, A. R., *Blast furnace and steel slag: production, properties, and uses*. Wiley: 1974.
55. Chaurand, P.; Rose, J.; Domas, J.; Bottero, J.-Y., Speciation of Cr and V within BOF steel slag reused in road constructions. *Journal of Geochemical Exploration* **2006,** *88*, (1), 10-14.
56. Chang, E. E.; Chiu, A.-C.; Pan, S.-Y.; Chen, Y.-H.; Tan, C.-S.; Chiang, P.-C., Carbonation of basic oxygen furnace slag with metalworking wastewater in a slurry reactor. *International Journal of Greenhouse Gas Control* **2013,** *12*, 382-389.
57. Huijgen, W. J. J.; Comans, R. N. J., Mineral CO2 Sequestration by Steel Slag Carbonation. *Environmental Science & Technology* **2005,** *39*, (24), 9676-9682.
58. Bayless, E. R.; Schulz, M. S., Mineral precipitation and dissolution at two slag-disposal sites in northwestern Indiana, USA. *Environmental Geology* **2003,** *45*, (2), 252-261.